Diamagnetism and beta in beam heated currentless plasmas of heliotron E

1986 Nucl. Fusion 26 1339

(http://iopscience.iop.org/0029-5515/26/10/007)

DIAMAGNETISM AND BETA IN BEAM HEATED CURRENTLESS PLASMAS OF HELIOTRON E

S. BESSHOU, C.E. THOMAS*, T. OHBA,
A. IIYOSHI, K. UO
Plasma Physics Laboratory,
Kyoto University,
Gokasho, Uji, Kyoto, Japan

ABSTRACT. The paper describes the first measurements of beta and diamagnetism in beam heated currentless plasmas of Heliotron E. These measurements were performed with a diamagnetic coil (1984–1985). The inferred volume average beta shows good agreement with the kinetic beta determined from the Thomson scattering electron temperature and density and the ion temperature profiles. A volume average beta of $\langle\beta_T\rangle^{DIA} = 0.7-0.9\%$ is obtained with 3.6 MW of neutral beam injection heating at 0.94 T. The observed maximum diamagnetic beta is close to and slightly below the value predicted by theoretical MHD predictions. The correlation between the diamagnetic beta and observed MHD fluctuations is discussed. The paper includes a general technique used to analyse the diamagnetism of the plasma confined in a helical heliotron device.

1. INTRODUCTION

The measurement of the plasma energy from diamagnetic signals is important in determining the volume averaged beta and the energy confinement time [1–6]. Moreover, for very high temperature and high density plasmas, the diamagnetic signals are stronger.

Recently, high beta plasmas in tokamaks have been studied in ISX-B [7, 8], Doublet III [9], and PDX [10]. The research concentrated on experimental investigation of limits on beta [22]. In helical systems with current, such as stellarators [11–13] and heliotrons [14, 15], the effect of the vacuum helical field on the diamagnetic signal should be considered in estimating the volume average beta value. In this report, we describe the initial measurements of the volume average beta value in beam heated currentless plasmas in the Heliotron E device [16]. The paper also presents a general method of analysing the plasma diamagnetism in the helical heliotron field.

2. DIAMAGNETIC SIGNALS FROM A PLASMA CONFINED IN THE HELICAL HELIOTRON FIELD

2.1. Diamagnetic flux in the helical heliotron device

The magnetic flux inside a single turn diamagnetic coil wound around the inside of a vacuum chamber is, on the assumption of a constant vacuum magnetic field, given by

$$\Delta\Phi^{DIAMAG}(t) = \Delta\Phi^{D} + \Delta\Phi^{P} + \Delta\Phi^{ST} \qquad (1)$$

where $\Delta\Phi^{D}$ is the true diamagnetic flux, $\Delta\Phi^{P}$ the paramagnetic flux due to the time varying toroidal current flowing along the helical self-transformed magnetic lines of force (these two terms determine the change in the flux in tokamaks) and $\Delta\Phi^{ST}$ the paramagnetic or diamagnetic flux due to the interaction of the helical heliotron field with the toroidal current flowing through the plasma (see Appendix). These quantities are given by

$$\Delta\Phi^{D} = -\frac{1}{2}\langle\beta_T\rangle^{DIA}\Phi_0 \qquad (2a)$$

$$\Delta\Phi^{P} = \frac{(\mu_0 I_p)^2}{8\pi B_{ho}} \qquad (2b)$$

* On leave from Oak Ridge National Laboratory, Oak Ridge, TN, USA.

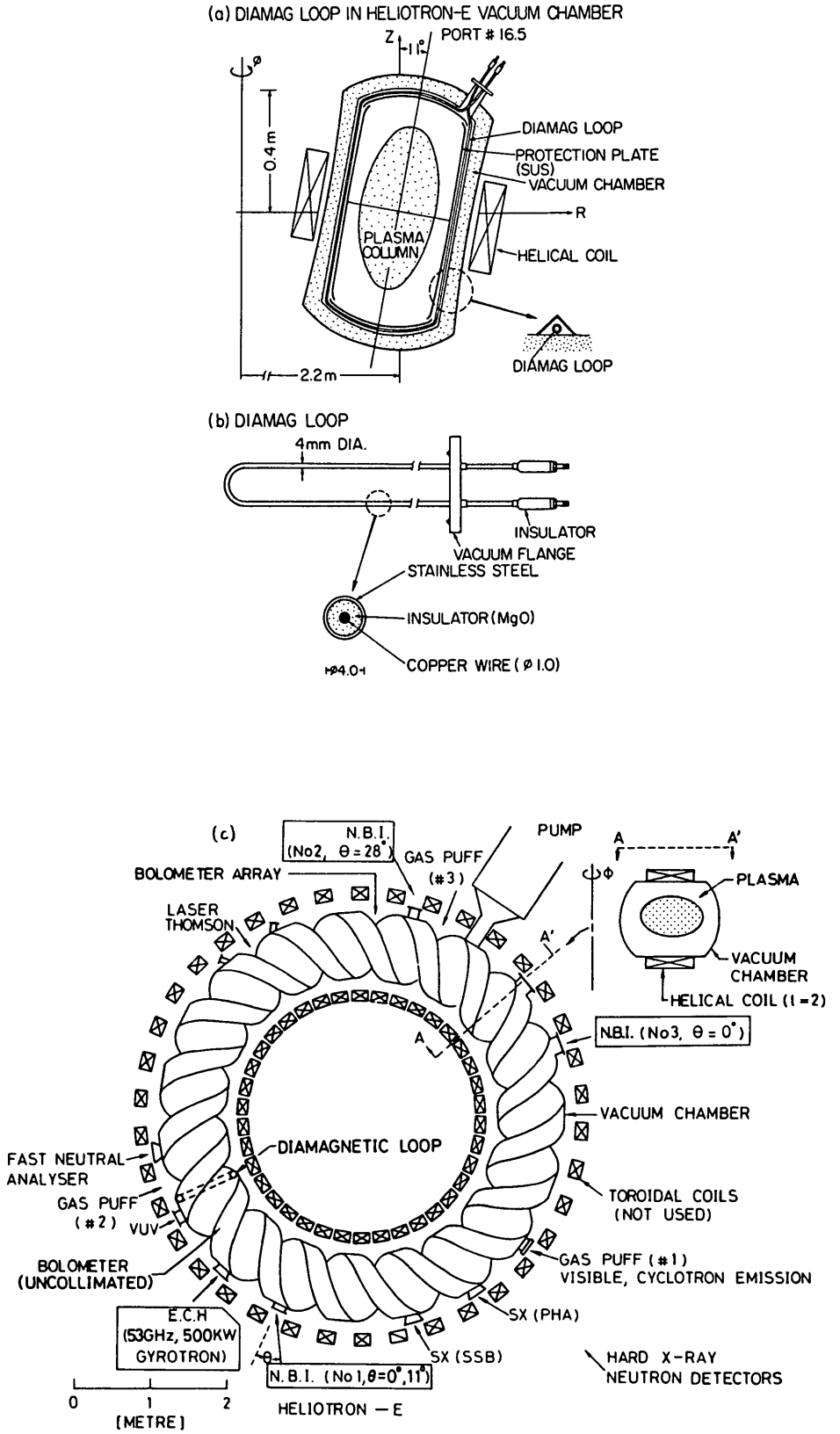

FIG. 1. (a) Poloidal cross-section of Heliotron E device. Single turn diamagnetic loop is located inside vacuum chamber; (b) construction details of diamagnetic loop; (c) top view of Heliotron E, as of September 1984.

$$\Delta\Phi^{ST} = \mu_0 \pi \int_0^{\bar{a}_p} \left(\frac{\bar{r}}{R}\right) \cdot \left(\frac{\iota(\bar{r})}{2\pi}\right) \cdot j_p(\bar{r}) \cdot \bar{r}^2 \, d\bar{r} \qquad (2c)$$

where $\langle\beta_T\rangle^{DIA}$ is the volume averaged beta value

$$\left(\equiv \left\langle nT / \frac{B_{ho}^2}{2\mu_0} \right\rangle\right)$$

Φ_0 the total flux in the plasma column ($\equiv \pi a_p^2 B_{h0}$), $\iota(r)$ the rotational transform angle and $j_p(\bar{r})$ the density of toroidal plasma current. We have used an averaged magnetic surface with radius $\bar{r}$. The average rotational transform angle of the Heliotron E device is given by

$$\iota \equiv \iota(\bar{r})/2\pi = 0.51 + 2.0\,(\bar{r}/a_p)^4 \qquad (3)$$

with $a_p = 0.2$ m and $R = 2.2$ m

2.2. Data analysis

Figure 1(a) shows the single turn diamagnetic loop located inside the vacuum vessel. Figure 1(b) presents construction details on the diamagnetic loop. A top view of the experimental setup is shown in Fig. 1(c). We have used two gated integrator circuits to integrate the diamagnetic loop signal and the helical coil current Rogowski coil signal.

We have calibrated the integrators by integrating the DC voltage from a mercury standard cell. Then we measured the magnetic flux (0.448 Wb) in a diamagnetic coil at $B_{h\phi 0} = 1.9$ T. The measured flux agrees, within 6%, with the calculated (Biot-Savart) flux (0.425 Wb) in a diamagnetic coil.

To separate the true diamagnetic signal from the signal due to the undulating confinement field, we have considered two coupling models: (a) coupling with the eddy current in a vacuum chamber, (b) the effect of redistribution of coil current in the helical conductor cross-sections [6].

Figure 2(a) shows the coupled components: helical conductor, torus vacuum chamber, diamagnetic loop, and plasma column are indicated. Figures 2(b) and (c) show the coupling models. In Fig. 2(b) we see the model of coupling between the helical coil current and the vacuum vessel eddy currents, while Fig. 2(c) represents the coupling model for current redistribution in the helical conductor. The Laplace transformation of the coupling equations is given by

$$\Delta\Phi(s)^{diamag} = \Phi(s)^{diamag\ coil} - A_{eff}\left(1 + \alpha_V \frac{s\tau_v}{1+s\tau_v} + \alpha_R \frac{s\tau_R}{1+s\tau_R}\right) I_h(s) \qquad (4)$$

where $\Phi(s)^{diamag\ coil}$ is the Laplace transform of the diamagnetic coil signal, τ_V the time constant of the eddy current in the vacuum chamber (4.2 ms), τ_R the time constant of redistribution in the helical coil conductor (97 ms), A_{eff}, α_V and α_R are the effective gain factors ($\alpha_V = 1.430$ and $\alpha_R = 0.197$), and $I_h(s)$ is the Laplace transform of the helical coil current.

The inverse Laplace transform is given by the convolution integrals,

$$\Delta\Phi(t)^{diamag} = \Phi(t)^{diamag\ coil} + \frac{\alpha_v}{\tau_v} A_{eff} \int_0^t I_h(\tau) \exp \times (-(t-\tau)/\tau_V) d\tau + \frac{\alpha_R}{\tau_R} A_{eff} \int_0^t I_h(\tau) \exp\ (-(t-\tau)/\tau_R) d\tau \qquad (5)$$

where $\Delta\Phi(t)^{diamag}$ is the compensated diamagnetic signal (after removal of the time varying helical field contribution). Introducing $\Delta\Phi(t)^{diamag}$ of Eq. (5) into Eq. (1) and using Eqs 2(a) to 2(c), we can calculate the true diamagnetic flux, $\Delta\Phi^D(t)$, and the volume average beta value $\langle\beta_T\rangle^{diamag}$.

The parameters α_v, α_R, τ_v, and τ_R are determined by a least squares fit minimizing

$$\chi^2 = \sum_{i=1}^{N} |\Delta\Phi(t_i)^{diamag}(\text{measured}) - \Delta\Phi(t_i)^{diamag}\ (\text{convolution})|^2 / \sigma_i^2$$

in field only shot (no plasma), where σ_i is the bit noise in $\Delta\Phi^{diamag}$(measured) due to the A-D convertor, and N is the sampling number.

The typical residual noise (0.02 mWb, 60 Hz) in the diamagnetic flux, $\Delta\Phi^{diamag}(t)$, remains. This residual noise corresponds to a 0.05% average beta in the case of a 0.94 T confining magnetic field.

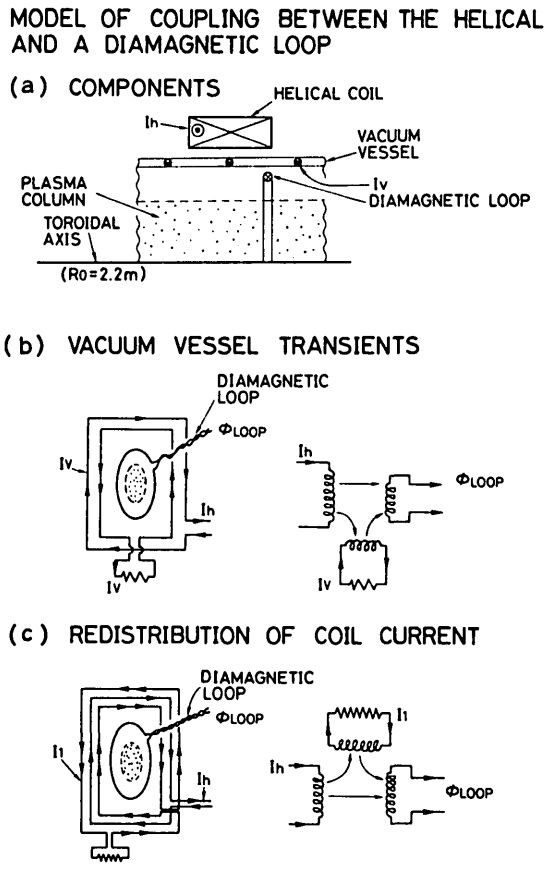

FIG. 2. Coupling models of diamagnetic measurements: (a) components (helical coil, vacuum chamber, plasma column, diamagnetic loop); (b) effect due to eddy current in vacuum chamber; (c) effect due to redistribution of coil current density in conductor.

3. EXPERIMENTAL RESULTS

3.1. Diamagnetic flux and beta values in beam heated currentless plasmas

A currentless plasma is produced by electron cyclotron resonance (53 GHz, 500 kW, 30 ms) and heated by neutral beam injection (NBI, 2.4 MW, $H^0 \rightarrow H^+$, three injectors) [17]. Figure 3 shows the analysed diamagnetic signal with a 2.4 MW injection at 0.94 T (low field). The diamagnetic flux increases during neutral beam injection. The maximum volume average beta value in this shot is 0.63%, the maximum plasma energy is 5.8 kJ, and the diamagnetic flux change was 0.37 mWb. The beta value reaches a maximum during the neutral beam pulse and then decreases.

The electron density increases monotonically with gas puffing. The central electron temperature at maximum beta (595 ms) is 350 eV. The decay time of the internal energy after neutral beam cutoff is about 6 ms. This value is comparable with the global energy confinement time, $\tau_E^G = W_p/P_{abs} = 4.8$ ms, where P_{abs} is the calculated absorbed neutral beam power (1.2 MW), which does not include orbit loss and charge exchange loss [18]. The total radiative loss at the end of NBI was about 0.9 MW, as is shown in Fig. 3.

Figure 4 shows the diamagnetic beta in a higher magnetic field ($B_{h0} = 1.9$ T). Beta continues increasing during the NBI pulse (2.4 MW through ports). The maximum volume average beta is 0.34%, and the plasma energy is 13 kJ. The time evolution of the kinetic average beta found from profile measurements is also plotted in Fig. 4. The kinetic average beta agrees well with the diamagnetic beta in a shot. The energy confinement time was $\tau_E = W_p/(P_{abs} - \partial W_p/\partial t) = 12$ ms at 1.9 T. This value is comparable with the decay time (10 ms) of the internal energy after the neutral beam

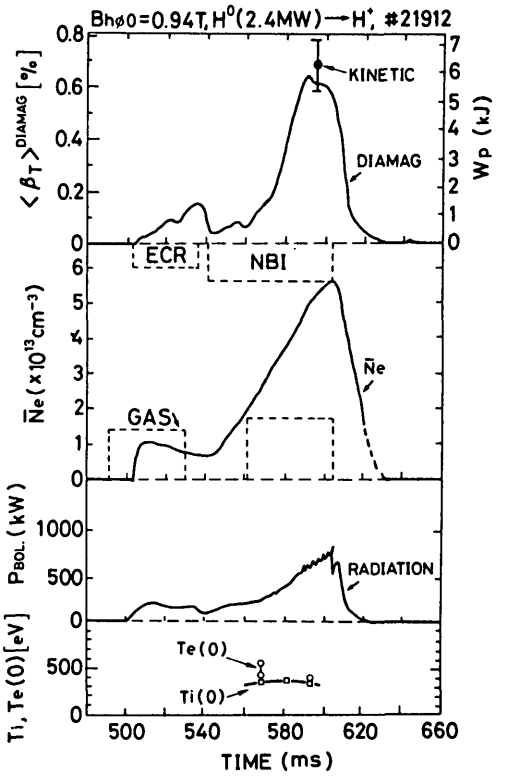

FIG. 3. Volume average beta, $\langle\beta_T\rangle^{diamag}$, and/or plasma energy versus time. Neutral beam power of 2.4 MW ($H^0 \rightarrow H^+$) is injected into hydrogen plasma with magnetic field of 0.94 T. Initial plasma is produced by second harmonic electron cyclotron resonance heating, using 53 GHz, 300 kW gyrotrons. Maximum beta value in this shot is 0.63%, plasma energy is 5.8 kJ at $N_e = 4 \times 10^{13}$ cm^{-3}.

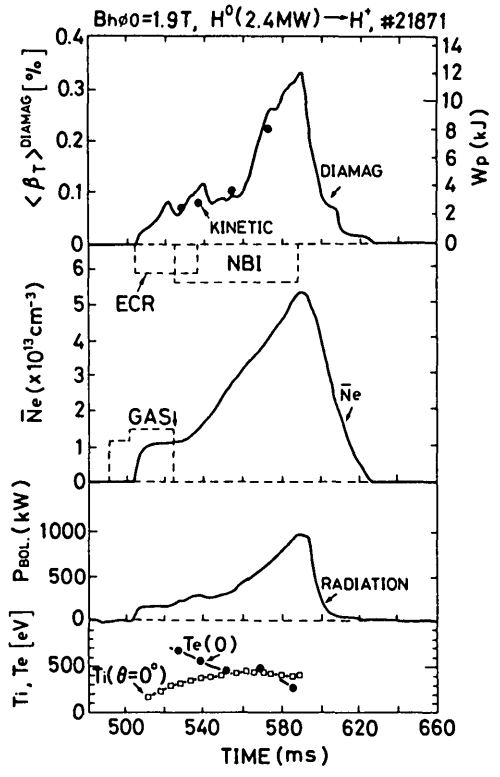

FIG. 4. Volume average beta, $\langle\beta_T\rangle^{diamag}$, and/or plasma energy versus time. Neutral beam power of 2.4 MW ($H^0 \rightarrow H^+$) is injected into hydrogen plasma with magnetic field of 1.9 T. Initial plasma is produced by fundamental electron cyclotron resonance heating using 53 GHz gyrotrons. Beta value of 0.34% is obtained at end of NBI pulse. Plasma energy is 12.6 kJ.

cutoff. By comparing with the low field (0.94 T) case in Fig. 3, we see that the energy confinement time is roughly proportional to the confinement magnetic field, $\tau_E \propto B_h^1$, with the same neutral beam injection power (2.4 MW) and similar density ($\bar{N}_e = (4-5) \times 10^{13}$ cm^{-3}).

The noise in our diamagnetic measurements is due to imperfect cancellation of ripple in the helical coil current (1%, 60 Hz). We have adjusted the time constant, τ_V, in Eq. (5) in order to minimize this noise ripple. In the diamagnetic signal of Fig. 4, we find ripple noise ($\Delta\langle\beta_T\rangle \approx 0.05\%$). This noise determines the actual error bar of our diamagnetic measurements.

3.2. Comparison of diamagnetic and kinetic betas

We shall now systematically compare the diamagnetic measurements with the kinetic measurements by Thomson scattering ($T_e(r)$) [19], and neutral particle analyser ($T_i(r)$) [20]. Figure 5(a) shows the electron and ion temperatures with 2.0 MW NBI at $\bar{N}_e = 5.5 \times 10^{13}$ cm^{-3}, and $B_{h\phi 0} = 0.94$ T (low field case). Assuming a parabolic profile of the electron density, we obtain a volume average kinetic beta, $\langle\beta_T\rangle^{kinetic}$, of 0.62%. The diamagnetic signal indicates a volume average beta, $\langle\beta_T\rangle^{diamag}$, of 0.59%.

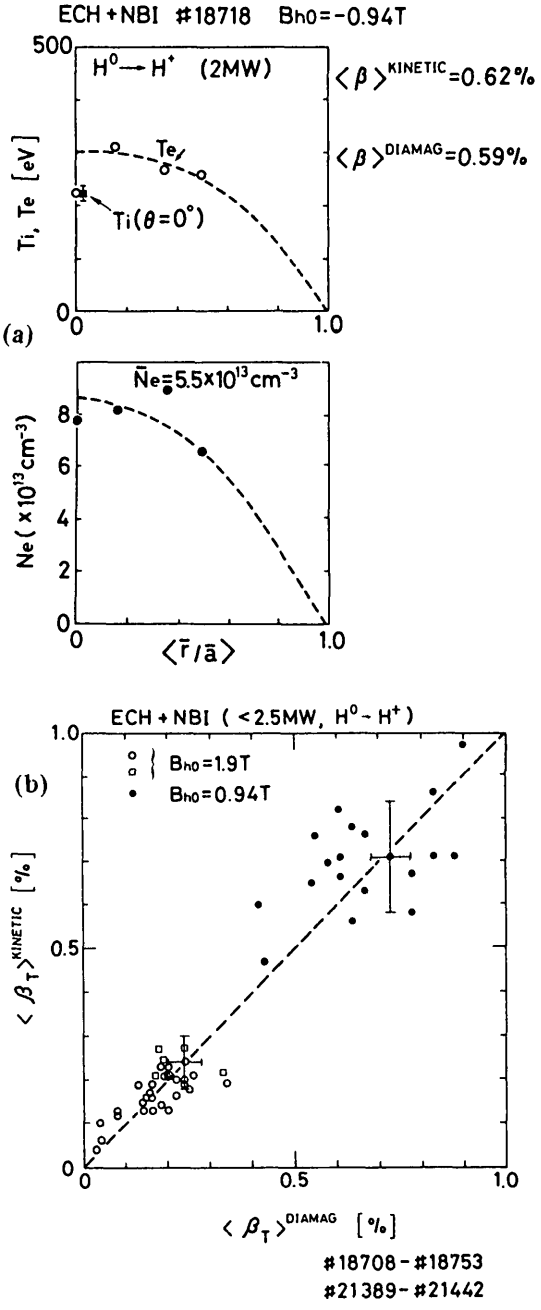

FIG. 5. (a) Kinetic measurement of volume average beta; electron temperature profile from Thomson scattering. Kinetic measurements indicate $\langle\beta_T\rangle^{kinetic} = 0.62\%$, while diamagnetic measurement indicates $\langle\beta_T\rangle^{diamag} = 0.59\%$.
(b) Kinetic volume average beta, $\langle\beta_T\rangle^{kinetic}$, versus diamagnetic beta, $\langle\beta_T\rangle^{diamag}$.

We have performed similar comparisons for about 50 shots with ECRH + NBI currentless plasmas. The kinetic beta values, $\langle\beta_T\rangle^{kinetic}$, are plotted as a function of the diamagnetic beta values, $\langle\beta_T\rangle^{diamag}$, in Fig. 5(b). These data show that kinetic and diamagnetic beta values agree within experimental errors, which, in the kinetic measurements, are due to statistical scatter in the electron temperature and density profiles.

There is a contribution of high energy particles to the plasma pressure. We thus agree that pressure anisotropy ($P_{\parallel} < P_{\perp}$) affects the measurements with nearly perpendicular neutral injectors. However, as is shown in Fig. 5(b), the diamagnetic beta agrees with beta by profile measurements (T_e, T_i, N_e) within experimental errors. If the beam component in $P_{\perp}$ is large, we notice a disagreement in the two independent measurements so that we may consider the anisotropy in the pressure to be virtually negligible.

3.3. Diamagnetic beta versus electron density

Figure 6 shows the volume average beta, $\langle\beta_T\rangle^{diamag}$, as a function of the electron density. The experiments were carried out with magnetic fields of 0.94 and 1.9 T respectively. The NBI power was 2.4 and 1.5 to 2 MW. These data show that the average beta value increases with the electron density. These increments are partially due to the increase of the absorbed beam power with the density.

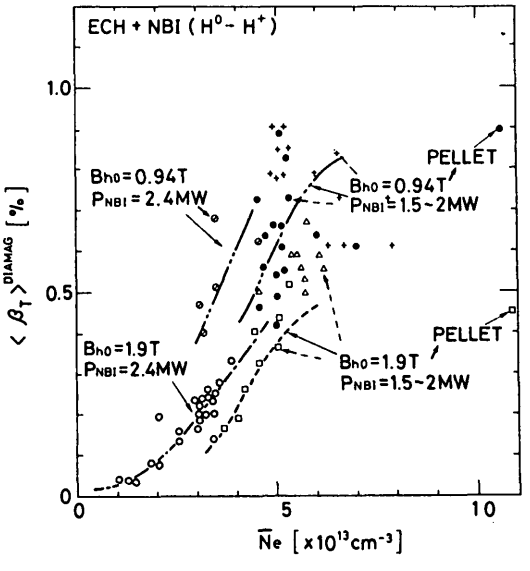

FIG. 6. Volume average beta, $\langle\beta_T\rangle^{diamag}$, versus line average electron density, $\bar{N}_e$. Black points and crosses are low field (0.94 T) experiments with NBI (1.5–2 MW). Triangles are high field case (1.9 T) with NBI (2 MW).

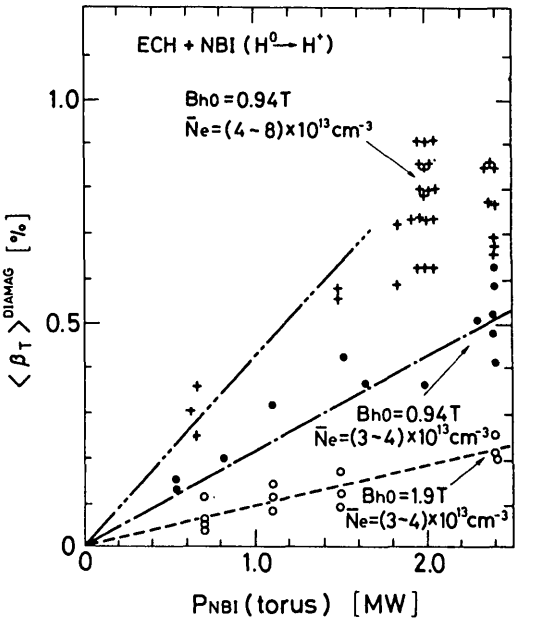

FIG. 7. Volume average beta, $\langle\beta_T\rangle^{diamag}$, versus NBI power into torus, P_{NBI}.

Above $\bar{N}_e = 5 \times 10^{13}$ cm^{-3}, the absorbed neutral beam power becomes 80% (or more) of the power injected into the torus. The maximum diamagnetic beta measured in 1984 and 1985 is about 0.9% at 0.94 T, with 2 MW of NBI. The data points with the high electron density ($\bar{N}_e = 1 \times 10^{14}$ cm^{-3}) in Fig. 6 are obtained with hydrogen pellet injection during NBI. These data show that beta, $\langle\beta_T\rangle^{diamag}$, plasma energy and energy confinement time saturate in the higher electron density regime ($\bar{N}_e \geqslant 5 \times 10^{13}$ cm^{-3}).

3.4. Diamagnetic beta versus NBI power

The diamagnetic beta is measured systematically, with fixed average density and varying neutral beam power.

Figure 7 shows the volume average beta value, $\langle\beta_T\rangle^{diamag}$, as a function of NBI power injected into the torus ($P_{NBI} \leqslant 2.4$ MW). An average beta value of 0.7 to 0.9% is obtained in the high density case ($\bar{N}_e = (4–8) \times 10^{13}$ cm^{-3}) at low field (0.94 T) with 2 MW ($H^0 \rightarrow H^+$) of NBI. In the low density ($\bar{N}_e = (2–3) \times 10^{13}$ cm^{-3}), high field (1.9 T) case, $\langle\beta_T\rangle^{diamag}$ was approximately proportional to the NBI power injected into the torus.

In low field case (0.94 T) with higher NBI power ($\geqslant$2 MW) and high electron density ($\bar{N}_e \geqslant 4 \times 10^{13}$ cm^{-3}) the diamagnetic beta does not always increase. Figure 8(a) shows the diamagnetic beta, $\langle\beta_T\rangle$, at 0.94 T with a neutral beam power of 3.6 MW at the ports. The maximum average beta is about 0.86% in this shot.

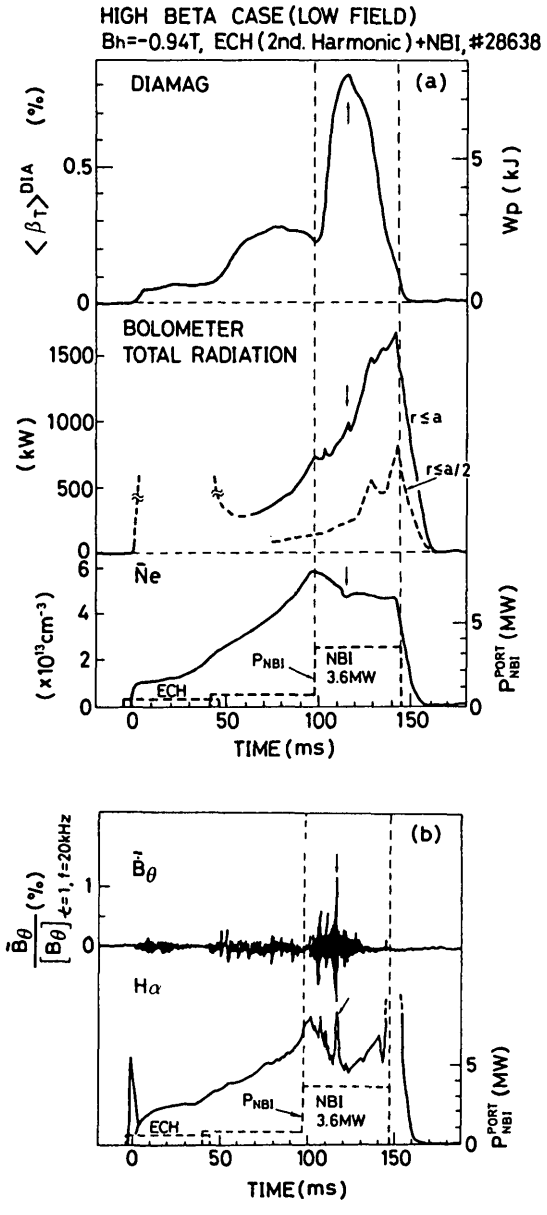

FIG. 8. Diamagnetic average beta at low field (0.94 T) with high neutral beam power (3.6 MW):
(a) diamagnetic average beta, total bolometric loss and average electron density;
(b) poloidal magnetic fluctuations ($\tilde{B}_\theta$) and H_α emission.

The diamagnetic beta is not in a steady state in the high beta (low field) experiments with higher NBI power ($\geq$1.5 MW). When we increase the neutral beam power above 2 MW, the obtainable maximum diamagnetic average beta is about 0.7–0.9%. The time before which maximum beta appears usually becomes shorter with increasing NBI power.

The energy confinement time depends therefore on $\langle\beta_T\rangle^{\text{diamag}}$ and P_{abs} in the medium electron density regime, $\bar{n}_e \geq 4 \times 10^{13}$ cm^{-3}. When the average beta is less than 0.5%, the energy confinement time does not strongly depend on the NBI power, which means that the plasma energy is proportional to the NBI power. However, when the average beta increases above 0.5–0.6%, the plasma energy is not always proportional to the NBI input power. This means that the energy confinement time decreases with the NBI power at $\langle\beta_T\rangle^{\text{diamag}} \geq 0.5\%$.

3.5. Diamagnetic average beta and magnetic fluctuations

To study the non-steady state of the diamagnetic average beta in the high beta (low field) case, the time evolution of diamagnetic beta is compared with poloidal magnetic fluctuations in Fig. 8(b). When the average diamagnetic beta increases above 0.5%–0.6%, poloidal magnetic fluctuations are detected by a calibrated Mirnov coil.

The fluctuations in $\tilde{B}_\theta$ are well correlated with soft X-ray (m = 1/n = 1) oscillations, the spikes in H_α and the ion saturation current [21].

The typical frequency of $\tilde{B}_\theta$ is 20–25 kHZ, and the normalized magnetic fluctuation, $\tilde{B}_\theta$ (wall, 20 kHz)/$B_\theta(\iota = 1)$, reaches 0.8%–1% with $\langle\beta_T\rangle^{\text{dia}} \geq 0.5$–0.6%, $\beta(0) \geq 1.8\%$ as is shown in Fig. 8(b), where $B_\theta(\iota = 1) = (0.7\ a/R)B_T$ is the calculated vacuum poloidal field at the $\iota = 1$ surface and is used for convenience. The energy loss to the wall is observed by a bolometer, as well as ion saturation current within 0.5 ms after the onset of the $\tilde{B}_\theta$ spikes, indicating that about 10% of the total plasma energy is lost in a large MHD spike. Thus, studying the steady power balance is difficult, because the total bolometric (radiative) loss increases with time and the plasma energy decreases in a long NBI pulse. These observations suggest that the enhancement of the radiation is a result of MHD fluctuation above a threshold beta (0.5%–0.6%) and of simultaneous particle loss to the wall.

Although strong gas puffing decreases the probability of incidence of bolometer spikes, poloidal magnetic fluctuations still appear when the diamagnetic average beta increases above 0.5–0.6%.

A strong MHD instability often occurs when the diamagnetic average beta $\langle\beta_T\rangle^{\text{dia}}$ is 0.8–0.9%. The arrow in Fig. 8(b) points at the corresponding instant of time. The poloidal magnetic fluctuations show good correlation with H_α emission in phase. After the occurrence of a strong MHD instability, the plasma energy (diamagnetic beta) decreases fast with a time constant of 2 to 3 ms and then decreases slowly with a longer time constant of 10 to 15 ms. The fast

decrease in plasma energy is, possibly, the result of the rapid energy loss ($-\partial W_p/\partial t = -200$ kW) by an interchange instability, where bolometric measurements detect the same amount of heat pulse (200 kW) at the wall, after a fast decay of beta [29–30]. The subsequent slow decrease of the plasma energy is the result of impurity accumulation due to the increase of impurity sources at the plasma boundary in the presence of a strong MHD instability.

It may be pointed out that $\langle\beta_T\rangle^{dia}$ – at constant neutral beam power – cannot be kept at that maximum value but decreases during the NBI pulse. This feature is quite similar to one revealed by a beta limit study in the ASDEX tokamak [22], where a soft disruption with a long decay time (100 ms) occurs at the Troyon limit of the diamagnetic average beta [23]. However, our maximum diamagnetic average beta available is much lower than the 'effective' Troyon limit ($2.8\, I_p\,[m]/(a\,[m]\cdot B[T]) = 3.1\%$, where the rotational transform at the boundary, $\iota(a) = 2.5$, the average minor radius a = 0.2 m, and a major radius of R = 2.2 m in Heliotron E are used to calculate the effective toroidal plasma current needed to produce the transform.

3.6. Measured beta and theoretical critical beta

Theoretical calculations of the critical beta in the Heliotron E device are now developing; they make use of different methods, and the conclusions arrived at generally agree [24–28]. The most serious instability for Heliotron E is the pressure driven m = 1, n = 1 interchange mode resonant at the $\iota = 1$ surface. Wakatani shows that the beta limit due to the ideal interchange mode seems to be $\beta_c(0) = 2.65\%$ for a pressure profile given by $(1-(r/a)^2)^2$ (thus, $\langle\beta_c\rangle = 0.88\%$) [24]. Below this value, as he shows, the m = 1/n = 1 mode is destabilized by finite resistivity. Shafranov shows, in his review paper, that without shift of the plasma column, the critical average beta ($\beta_0/2$) for stability is about 1% [25]. Anania and Johnson indicate the onset of an n = 1 instability for $\langle\beta\rangle \gtrsim 1\%$, by utilizing stellarator expansion and free boundary code [26]. Bauer, Betancourt and Garabedian show that the critical average beta for the first stability region is 2% and find a second stability region for 5% [27].

Recently, Rewoldt and Johnson have calculated the stability limit of the Heliotron E currentless plasmas, $\langle\beta_c\rangle = 1.1-1.4\%$, by using the stellarator expansion method [28]. They have used rather broad pressure profiles to calculate the theoretically obtainable higher average beta value in Heliotron E. Our diamagnetic measurements of average beta agree with their theoretical conclusion, because the measured highest diamagnetic beta (0.8–0.9%) available in Heliotron E is close to or slightly below the theoretically calculated value.

4. DISCUSSIONS AND SUMMARY

In this experiment, we have used the diamagnetism of a plasma to measure its energy content and its volume average beta, for the first time, in a helical heliotron toroidal plasma confining device. The fact that the volume average diamagnetic beta shows good proportionality with the kinetic measurements demonstrates its usefulness for measuring beta (continuously) in currentless Heliotron E plasmas.

The diamagnetic volume average beta, $\langle\beta_T\rangle^{dia}$, is roughly proportional to the NBI power in the low beta ($\langle\beta_T\rangle^{dia} \leqslant 0.5\%$) region. In this region, the global energy confinement time is proportional to the confining helical heliotron magnetic field.

The maximum diamagnetic average beta $\langle\beta_T\rangle^{dia}$ available in Heliotron E is 0.8–0.9% with low field (0.94 T) and high neutral beam power at the ports (3.6 MW). This observed maximum average beta is close to or slightly below the value calculated by theoretical stellarator expansion studies on the Heliotron E beta limit.

MHD fluctuations usually appear when the diamagnetic average beta becomes 0.5–0.8%. The poloidal magnetic fluctuations with hard spikes show good correlation with the particle and energy losses to wall (i.e. H_α and bolometer spikes). In this case, the diamagnetic beta usually decreases during the NBI pulse. The pressure driven interchange instability, which is predicted by the stellarator expansion theories, explains MHD fluctuations versus diamagnetic average beta.

The finite plasma resistivity usually decreases the theoretical critical beta limit of stability. Thus, we believe that the observed maximum average beta available is in the range covered by the available stellarator expansion theories. Therefore, we assume that optimization studies on the highest achievable beta for helical systems are quite promising and encouraging, by using the current MHD theories.

This paper does not, of course, maintain reporting on a perfect experimental study of the beta limit in Heliotron E. We expect a further increase in the diamagnetic beta by reducing impurity radiation, by shifting plasma column outwards or by using toroidal coils. In such cases, we shall need a further compensa-

tion of the diamagnetic signals, by a technique that is similar to that described in Section 2 of this paper.

We believe that our high beta experiment with diamagnetic measurements in Heliotron E is new and that it is worth emphasizing the necessity of studies of high beta plasma physics in helical systems.

Appendix

THE INDUCED TOROIDAL FLUX, $\Delta\Phi^{ST}$, DUE TO THE COUPLING BETWEEN THE HELICAL HELIOTRON FIELD AND THE TOROIDAL PLASMA CURRENTS

In experiments in toroidal devices with a rotational transform in the vacuum helical field, e.g. stellarators and heliotrons, the diamagnetic coil will pick up any other signal due to toroidal plasma currents flowing along the helical field lines.

Now, from Maxwell's equation, we have the equation for the θ-(poloidal) components,

$$\frac{\partial B_r}{\partial z} - \frac{\partial B_z}{\partial r} = \mu_0 j_\theta \tag{A1}$$

where j_θ is the poloidal component of the plasma current flowing along the helical field and z is the toroidal co-ordinate.

Assuming $\partial B_r/\partial z = 0$, we have

$$\frac{\partial B_z}{\partial r} = -\mu_0 j_p \frac{B_\theta}{B_z} \tag{A2}$$

where we use $j_\theta = j_p B_\theta / B_z = j_p \epsilon_t \iota/2\pi$. Multiplying by πr^2 and integrating Eq. (A2) by parts, we have

$$\pi a_p^2 B_z(\bar{a}_p) - \int_0^{\bar{a}_p} B_z(\bar{r})\, 2\pi \bar{r}\, d\bar{r}$$

$$= -\mu_0 \pi \int_0^{\bar{a}_p} j_p \left(\frac{\bar{r}}{R}\right)\left(\frac{\iota}{2\pi}\right)\bar{r}^2\, d\bar{r} \tag{A3}$$

The left hand side of this equation is the induced toroidal flux, $\Delta\Phi^{ST}$, due to the helical plasma current. Including the sign of the flux in j_p, we have

$$\Delta\Phi^{ST} = \mu_0 \pi \int_0^{\bar{a}_p} j_p \left(\frac{\bar{r}}{R}\right)\left(\frac{\iota}{2\pi}\right)\bar{r}^2\, d\bar{r} \tag{A4}$$

This term is the third term of Eq. (1).

Assuming that the axial component of the toroidal plasma current density distribution, j_p, is given by

$$j_p = j_0 \left\{1 - \left(\frac{\bar{r}}{a_p}\right)^2\right\}^S \tag{A5}$$

and using Eq. (3a) for $\iota(\bar{r})$, we have numerically the normalized induced flux, $2\Delta\Phi^{ST}/\Phi_0$ as a function of the normalized current, $2\mu_0 I_p/\pi R B_{h0}$,

$$2\frac{\Delta\Phi^{ST}}{\Phi_0} = K\left\{2\frac{\mu_0 I_p}{\pi R B_{h0}}\right\} \tag{A6}$$

Here,

$$\Phi_0 \equiv \pi \bar{a}_p^2 B_{h0} \tag{A7}$$

$$K \equiv \left[\frac{1}{2}\int_0^1 (0.51 + 2\chi^4)(1-\chi^2)^S \chi^3\, d\chi\right] \Bigg/ \left[\int_0^1 (1-\chi^2)^S \chi d\chi\right] \tag{A8}$$

where K is a number determined by the current profile: K = 0.375 for S = 0, K = 0.183 for S = 1, and K = 0.113 for S = 2.

Figure 9(a) illustrates Eq. (A6), showing the normalized induced toroidal flux as a function of the normalized current at several current profiles. These diagrams show the possible uncertainty in the beta value, $\langle\beta_T\rangle^{diamag}$, due to the variation of the current profile. The toroidal current is usually less than 3 kA in the ECH plus NBI case [31, 32]. The corresponding normalized induced toroidal flux, $2\Delta\Phi^{ST}/\Phi_0$, at 0.94 T is less than 0.05% as is shown by A in Fig. 9(a). The tokamak term (paramagnetic), $2\Delta\Phi^{P}/\Phi_0$, is much smaller than the stellarator term as is shown by the broken line in Fig. 9(a). Therefore, the effect of the low toroidal current ($\leqslant$3 kA) on the diamagnetic signal is small when beta is around 1%.

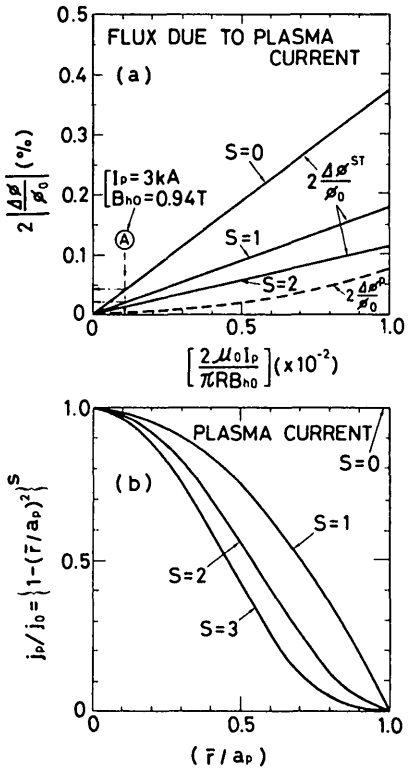

FIG. 9. (a) Induced toroidal flux due to coupling between helical heliotron field and toroidal plasma current for several values of S. $2|\Delta\Phi/\Phi_0|$ is normalized toroidal flux induced by plasma current; $2|\Delta\Phi^{ST}/\Phi_0|$ is toroidal flux induced by coupling of helical field and plasma current; $2|\Delta\Phi^{P}/\Phi_0|$ is normalized paramagnetic flux due to plasma current; (b) plasma current distribution profile for several values of S.

ACKNOWLEDGEMENTS

The authors wish to express their gratitude to the entire Heliotron group and, in particular, to Professor O. Motojima for arranging the experiments. They thank T. Mutoh and Y. Ijiri for sharing their electron density data, S. Sudo for the Thomson scattering data and H. Zushi for the ion temperature data. Thanks are also due to Dr. Neilson for helpful comments. This work was partially supported by a grant-in-aid for scientific research offered by the Japanese Ministry of Education under No. 59780007.

REFERENCES

[1] UO, K., Plasma Phys. **7** (1965) 123.
[2] UO, K., Phys. Fluids **8** (1965) 384.
[3] RAZUMOVA, K.A., Plasma Phys. **8** (1966) 791.
[4] ROTHMAN, M.A., Plasma Phys. **10** (1968) 86.
[5] HUTCHINSON, I.H., Plasma Phys. **18** (1976) 246.
[6] NEILSON, G.H., Diamagnetic Measurements on ISX-B: Method and Results, Oak Ridge National National Laboratory Rep. ORNL/TM-8767 (1983).
[7] NEILSON, G.H., Nucl. Fusion **23** (1983) 285.
[8] SWAIN, D.W., Nucl. Fusion **21** (1981) 1409.
[9] BURREL, K.H., STAMBAUGH, R.D., ANGEL, T.R., ARMENTROUT, C.J., BLAU, F.P., et al., Nucl. Fusion **23** (1983) 536.
[10] DAVIS, S.L., Plasma Phys. **25** (1983) 189.
[11] MIKHAILOV, M.I., Sov. J. Plasma Phys. **6** (1980) 25.
[12] ANDRYUKHINA, E.D., FEDYANIN, O.I., Sov. J. Plasma Phys. **3** (1977) 447.
[13] MIYAMOTO, K., Nucl. Fusion **18** (1978) 243.
[14] UO, K., J. Phys. Soc. Jpn. **16** (1961) 1380.
[15] UO, K., Plasma Phys. **13** (1971) 243.
[16] UO, K., IIYOSHI, A., OBIKI, T., MOTOJIMA, O., MORIMOTO, S., et al., in Plasma Physics and Controlled Nuclear Fusion Research 1982 (Proc. 9th Int. Conf. Baltimore, 1982), Vol. 2, IAEA, Vienna (1983) 209.
[17] UO, K., IIYOSHI, A., OBIKI, T., MOTOJIMA, O., MORIMOTO, S., et al., Nucl. Fusion **24** (1984) 1551.
[18] HANATANI, K., WAKATANI, M., UO, K., Nucl. Fusion **21** (1981).
[19] SUDO, S., KONDO, K., MUTOH, T., Jpn. J. Appl. Phys. 22 (1983) 485.
[20] ZUSHI, H., NAKASHIMA, K., KONDO, K., IIYOSHI, A., UO, K., J. Phys. Soc. Jpn. **51** (1982) 2673.
[21] HARRIS, J.H., MOTOJIMA, O., KANEKO, H., BESSHOU, S., ZUSHI, H., et al., Phys. Rev. Lett. **53** (1984) 2242.
[22] KEILHACKER, M., Annual Report (1985), Max-Planck-Institut für Plasmaphysik.
[23] TROYON, F., GRUBER, R., SAURENMANN, H., SEMENZATO, S., SUCCI, S., Plasma Phys. Controll. Fusion **26** (1984) 209.
[24] WAKATANI, M., IEEE Trans. Plasma Sci. **9** (1981) 243.
[25] SHAFRANOV, V.D., Phys. Fluids **24** (1983) 357.
[26] ANANIA, G., JOHNSON, J.L., Phys. Fluids **26** (1983) 3070.
[27] BAUER, F., BETANCOURT, O., GARABEDIAN, P., Magnetohydrodynamic Equilibrium and Stability of Stellarators, Springer-Verlag (1984).
[28] REWOLDT, G., JOHNSON, J.L., Plasma Phys. Controll. Fusion **27** (1985) 1203.
[29] BESSHOU, S., MORIMOTO, S., MOTOJIMA, O., MUTOH, T., SATO, M., et al., Nucl. Fusion **26** (1986) 114.
[30] BESSHOU, S., MORIMOTO, S., MOTOJIMA, O., KANEKO, H., KONDO, K., et al., in Controlled Fusion and Plasma Heating (Proc. 13th Eur. Conf. Schliersee, 1986), Tu-60.
[31] BESSHOU, S., MOTOJIMA, O., SATO, M., OBIKI, T., IIYOSHI, A., UO, K., Plasma Phys. **26** (1984) 565.
[32] BESSHOU, S., MOTOJIMA, O., SATO, M., IIYOSHI, A., UO, K., et al., Toroidal Plasma Current Driven in Electron Cyclotron Resonance Heating in Heliotron E, Plasma Physics Lab. Kyoto University Rep. PPLK-R-4 (Nov. 1985).

(Manuscript received 20 March 1985
Final manuscript received 23 June 1986)